Strong adhesion by regulatory T cells induces dendritic cell cytoskeletal polarization and contact-dependent lethargy

Jiahuan Chen,[1,2]* Anutosh Ganguly,[3]* Ashley D. Mucsi,[3] Junchen Meng,[1,2] Jiacong Yan,[1,2] Pascal Detampel,[3] Fay Munro,[3] Zongde Zhang,[1,2] Mei Wu,[1,2] Aswin Hari,[3] Melanie D. Stenner,[3] Wencheng Zheng,[1] Paul Kubes,[6] Tie Xia,[1,2] Matthias W. Amrein,[4,5,6] Hai Qi,[1,2] and Yan Shi[1,2,3,6]

[1]Tsinghua-Peking Center for Life Sciences and [2]Institute for Immunology, School of Medicine, Tsinghua University, Beijing 10084, China
[3]Department of Microbiology, Immunology, and Infectious Diseases and [4]Department of Cell Biology, Cumming School of Medicine, University of Calgary, Calgary, T2N 1N4 Alberta, Canada
[5]Department of Anatomy and [6]Snyder Institute, Cumming School of Medicine, University of Calgary, Calgary, Alberta T2N 1N4, Canada

Dendritic cells are targeted by regulatory T (T reg) cells, in a manner that operates as an indirect mode of T cell suppression. In this study, using a combination of single-cell force spectroscopy and structured illumination microscopy, we analyze individual T reg cell–DC interaction events and show that T reg cells exhibit strong intrinsic adhesiveness to DCs. This increased DC adhesion reduces the ability of contacted DCs to engage other antigen-specific cells. We show that this unusually strong LFA-1–dependent adhesiveness of T reg cells is caused in part by their low calpain activities, which normally release integrin–cytoskeleton linkage, and thereby reduce adhesion. Super resolution imaging reveals that such T reg cell adhesion causes sequestration of Fascin-1, an actin-bundling protein essential for immunological synapse formation, and skews Fascin-1–dependent actin polarization in DCs toward the T reg cell adhesion zone. Although it is reversible upon T reg cell disengagement, this sequestration of essential cytoskeletal components causes a lethargic state of DCs, leading to reduced T cell priming. Our results reveal a dynamic cytoskeletal component underlying T reg cell–mediated DC suppression in a contact-dependent manner.

INTRODUCTION

Suppressive functions of regulatory T (T reg) cells are multifaceted (Shevach, 2009). In one modality, T reg cells indirectly dampen immune activation through suppression of DCs. This inhibition requires binding between the two cell types, and the structural basis for this high-strength binding is adhesion molecules, particularly LFA-1 (Onishi et al., 2008; Tran et al., 2009), assisted in some cases by neuropilin-1 (Sarris et al., 2008; Hansen et al., 2012; Delgoffe et al., 2013) and co-stimulatory molecules (Lim et al., 2012). Several proposed mechanisms of T reg cell–mediated DC inhibition are built on the physical association of DCs and T reg cells. For instance, spatial proximity is essential for steady ligation of CD86 on the DCs by T reg cells that results in production of indoleamine 2,3-dioxygenase. The latter creates metabolic constraint by converting tryptophan to kynurenine in DCs (Grohmann et al., 2002). For two additional proposed models of T reg cell suppression, Granzyme B–mediated APC cytolysis and plasma membrane CD39/CD73-catalyzed generation of cAMP-inducing adenosine also require close contact (Zhao et al., 2006; Deaglio et al., 2007). Wing et al. (2008) reported that T reg cell–specific deficiency of CTLA-4 leads to a loss of T reg cell suppression in BALB/c mice. It was found that CD86 was pulled from DCs by CTLA-4 expressed on T reg cells. CD86 was then internalized by the T reg cells for degradation (Cederbom et al., 2000; Serra et al., 2003; Misra et al., 2004). However, in C57BL/6 mice, CTLA-4 was not found to be critical for T reg suppression (Paterson et al., 2015).

Amid consequences of the close contact, LFA-1–dependent binding between T reg cells and DCs operates as a biophysical interference. T reg cells appear to intercept DCs in their migration in vivo (Matheu et al., 2015). Live cell imaging indicates that the presence of T reg cells extends the number of CD4 T cells with higher motility in LNs, suggesting a reduced probability and duration of contact between conventional T (T conv) cells and DCs (Tadokoro et al., 2006; Tang et al., 2006). Questions arise as to whether the tight adhesion between DCs and T reg cells can directly affect DCs' ability to interact with cognate T cells. Whether the contact by T reg cells introduces a physical barrier to DCs in their antigen presentation to T conv cells has not been experimentally tested thus far, although, intuitively, such an interference might account for the suppressive effect of T reg cells. In this study, we show that LFA-1 on T reg cells displays an unusual high strength binding as a result of reduced calpain activities essential for integrin recycling. This strong adhesion alters the cytoskeleton of DCs, limiting the latter's ability to physically

*J. Chen and A. Ganguly contributed equally to this paper.

Correspondence to Yan Shi: yanshi@biomed.tsinghua.edu.cn

Abbreviations used: AFM, atomic force microscopy; IS, immunological synapse; PFA, paraformaldehyde; SCFS, single-cell force spectroscopy; SIM, structured illumination microscopy.

The Rockefeller University Press $30.00
J. Exp. Med. 2017 Vol. 214 No. 2 327–338
https://doi.org/10.1084/jem.20160620

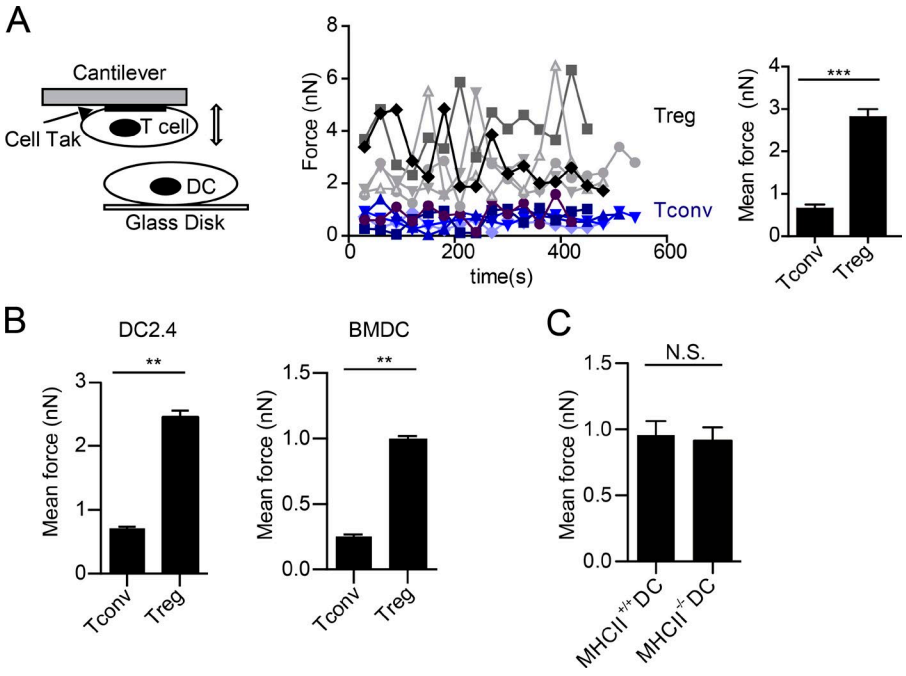

Figure 1. **T reg cells show strong binding to DCs.** (A) A schematic diagram for AFM-SCFS assay setup (left) and SCFS force readings for T cells of indicated types adhering to DC2.4 cells (middle). Black or gray. T reg cell (5); other colors, T conv (5). All data points (dots in the middle) from five independent DC-T cell pairs for each condition, collected on the same day, were used to generate the bar graph to the right. The data presented (middle and right) are collectively considered as one experiment. Error bars are SEM. All the force graphs henceforth used the identical analysis to show all data points collected from all T–DC pairs of each condition in one experiment. For all subsequent figures involving SCFS, at least 14 force readings were collected for each T–DC pair, and a minimum of three independent T–DC pairs were performed and analyzed for each condition. (B) Mean forces of T cells of indicated types adhering to DC2.4 cells (left) or BMDCs (right). (C) Mean forces of T reg cells adhering to wild-type and MHC class II–deficient BMDCs. **, $P < 0.01$; ***, $P < 0.001$; N.S., not significant. Each panel is representative of at least five independent experiments.

interact with cognate T conv cells. These results propose a reversible and probabilistic restraining mechanism to control the scale of T conv activation and reveal a biophysical aspect of T reg cell biology.

RESULTS AND DISCUSSION

To gain insight into the mechanism underlying T reg cell adhesion to DCs, we resorted to Atomic Force Microscopy (AFM)-based single-cell force spectroscopy (SCFS). This method allows us to directly measure the adhesion force between individual pairs of interacting cells in vitro (Ng et al., 2008; Lim and Ricciardi-Castagnoli, 2012; Fig. S1), as exemplified in Fig. 1 A. Freshly isolated T reg cells were difficult to glue to the AFM cantilevers; they were treated with IL-2 overnight for efficient mounting (Fig. 1 A). When cantilever-mounted T reg cells were allowed to contact BMDCs or DC2.4 cells on the glass disk, exceedingly strong binding forces were detected between T reg cells and the two types of DCs (Fig. 1 B). In contrast to typical cellular contacts, in general, requires only a force <200 pN to rupture (Helenius et al., 2008), T reg cell–DC adhesion required forces in the nanonewton range to pull apart. Although T reg cells adhered to BMDCs and DC2.4 cells with somewhat different intensities, a consistent four- to fivefold difference was always seen when T reg and T conv cells were compared. We compared the adhesion intensities to DCs derived from wild-type or class II MHC–deficient BM by force spectroscopy and found no apparent differences (Fig. 1 C). In this issue, Yan et al. describes the need for in vivo IL-2 to sustain the prolonged engagement between T reg and T cells, MHC class II is also found to be nonessential for this strong adhesion. Collectively, these results suggest that this high binding intensity is likely intrinsic to T reg cells and is antigen-independent.

LFA-1 has long been implicated in antigen-specific T reg cell–DC interactions (Onishi et al., 2008; Tran et al., 2009; Au-Yeung et al., 2010; Herman et al., 2012) and plays an essential role in T reg cell–mediated protection of colitis (Wohler et al., 2009). In replicating the outcomes of Wohler et al. (2009), we found that $CD45RB^{high}$ $CD4^+$ T cell transfer-mediated colitis in Rag1-deficient mice was ameliorated by co-transfusion of $CD25^+$ wild-type CD4 T cells, but not by their LFA-1–deficient counterpart (unpublished data), suggesting LFA-1 on T reg cells is required for their suppression. We sought to determine the role of LFA-1 in T reg cell–DC adhesion. As measured by AFM-SCFS, $Cd11a^{-/-}$ T reg cells could not adhere to DCs as strongly as wild-type T reg cells, exhibiting forces similar to those between T conv cells and DCs (Fig. 2 A). When $Icam1^{-/-}$ and $Icam1^{+/+}$ BMDCs were compared in the same assay, T reg cells strongly adhered only to the ICAM-1–sufficient DCs (Fig. 2 A). Therefore, LFA-1 and ICAM-1 are essential for the T reg cell–DC adhesion. Importantly, this strong LFA-1–dependent T reg cell–DC adhesion did not simply result from heightened LFA-1 expression by T reg cells, because the surface LFA-1 level on T reg cells was heterogeneous, but was not higher than freshly activated T conv cells ($CD25^+$ population in T conv cells treated with anti-CD3 and -CD28; Fig. 2 B). Furthermore, when tested for adhesion to an ICAM-1–coated inert surface, T reg cells also exhibited a much higher level of binding (Fig. 2 C), suggesting that LFA-1 molecules on T reg cells are in a unique struc-

tural or kinetic state that imparts increased adhesiveness. We ruled out involvement of arginine residue ADP-ribosylation, a mechanism previously suggested for LFA-1 affinity regulation in CD8 T cells (Okamoto et al., 1998; Fig. 2 D). To exclude the possibility that LFA-1 on T reg cells was in a constitutively high-adhesion state, we used human T reg cells for analysis, as anti–open-conformation LFA-1 antibodies are not available for mouse. The IL-2 treatment that was required to have higher binding to human APCs (PMA-stimulated THP-1) did not alter the staining, and no open-conformation LFA-1 was found on T reg cells (Fig. 2 E). This was in contrast with stimulation with Mg^{2+} while chelating Ca^{2+}, a method used to induce the open conformation (Stewart et al., 1998), where the increased staining by this antibody was readily seen (Fig. 2 E). To establish strong adhesion, integrin molecules must be connected to cortical cytoskeleton via linker proteins such as talin, an anchoring mechanism against pulling perpendicular to the membrane (Jiang et al., 2003; Tadokoro et al., 2003; Kim et al., 2011). Conversely, de-adhesion or release of integrin binding involves proteolytic cleavage of the talin molecule by Ca^{2+}-dependent nonlysosomal calpain family proteases (Stewart et al., 1998; Svensson et al., 2010). Because calpain family of proteases contains ∼20 members (Goll et al., 2003), we used a fluorescence substrate CMAC to measure their summed enzymatic activities by FACS. Interestingly, in this end-point assay, fewer T reg cells showed substrate conversion, resulting in overall lower calpain activities (Fig. 2 F). This stochastically reduced the likelihood of substrate conversion may reflect a regulatory event in calpain activities different in T reg and T conv cells, such as Ca^{2+} oscillation, subunit availability, or calpain autolysis (Dustin, 2008; Svensson et al., 2010). As CMAC assay is rapid, its stochastic reduction may reflect overall lower calpain activities in T reg cells over time. When T reg cells were treated with calpeptin, a pan-calpain competitive inhibitor, their adhesion to DCs was further increased (Fig. 2 G). The same treatment also increased T conv adhesion to DCs, but did not make *Cd11a*$^{-/-}$ T reg cells more adhesive (Fig. 2 G). Therefore, a reduced ability to release ligand-engaged, high-binding LFA-1 is likely responsible for the strong adhesion between T reg cells and DCs. To reveal the specific calpain species responsible for LFA-1 turnover, lentivirus-mediated expression of m-calpain or its constitutively active mutant was transfected into T reg cells. These treatments reduced T reg cell adhesion to DC2.4, whereas μ-calpain overexpression had no effect (Fig. 2 H). The same m-calpain (or its constitutively active version)-transduced T reg cells had reduced suppression of OT-II division stimulated by OVA-pulsed DCs (Fig. 2 I). The role of m-calpain in mediating LFA-1 turnover is in line with a previous study (Svensson et al., 2010). Nevertheless, it should be noted that the m-calpain transfection did not completely reverse the proliferation to the extent of no T reg cell control, suggesting that our model does not account for all aspects of T reg cell inhibitory effects. The associated biological impact will need future quantification.

To examine whether the strong adhesion by T reg cells would interfere with engagement of the same DCs by antigen-specific T conv cells, a new SCFS technique must be developed to study force interactions in a triple cell setup. This had not been possible because of the noise in force reading when a T cell was used to contact a DC already in association with another T cell. We successfully developed a new protocol after repeated attempts. This assay involves putting one T cell onto one side of a sufficiently large DC and recording forces generated by another T cell approaching the DC from the other side, with the two sides separated by the DC nucleus. Using this protocol, we measured the interacting force between OT-II T cells and OVA-presenting DCs that were either free or engaged by polyclonal T reg cells (Fig. 3 A). As shown in Fig. 3 A, whereas OT-II cells strongly adhered to OVA-presenting, T reg cell–free DCs, they failed to adhere to the DCs coupled by T reg cells, indicating that T reg cells acutely impaired DCs for simultaneous interactions with antigen-specific $CD4^+$ T cells. This interference of DC–T interaction was minimal when the DC was engaged by a T conv cell (Fig. 3 A). The binding forces of OT-II cells to OVA-presenting DCs that were already in contact with activated OT-II cells were also not significantly different compared with DCs free of any contact (Fig. 3 A). Taking advantage of the strong adherence of DC2.4 cells to the glass disk, we physically flushed T reg cells off DCs by pipetting with media and tested whether the functional impairment could persist (Fig. 3 B). When an OT-II cell was brought into contact with a T reg cell–experienced DC immediately after dislodging of the T reg cell, the binding force between the OT-II T cell and the DC was initially very low, and over a subsequent period of 3–5 min, steadily recovered to the normal level of antigen-specific T cell–DC adhesion (Fig. 3 B). Therefore, T reg cells can, in a contact-dependent manner, reversibly impair individual DCs for simultaneous adhesion by antigen-specific T conv cells in vitro. Constitutively expressed by T reg cells, CTLA-4 has been shown to be important for DC-targeted suppression in BALB/c mice, a conclusion drawn exclusively from analyses of antigen-specific T reg cells (Wing et al., 2008; Qureshi et al., 2011). We tested whether CTLA-4 would be involved in the antigen-independent T reg cell–mediated suppression. As shown in Fig. 3 C, *Ctla4*$^{-/-}$ T reg cells adhered to DCs strongly and could still inhibit adhesion between OT-II T cells and OVA-pulsed DCs. In our system, CTLA-4–deficient T reg cells suppressed OT-II proliferation to a degree similar to that of wild-type T reg cells (Fig. 3 D). These data indicate that CTLA-4 is not required for the strong adhesion between T reg cells and DCs or qualitatively responsible for transmitting signals that trigger the lethargic state.

Although T cells can be activated by antigen-positive APCs via sequential short contacts (Dustin, 2008), some T cells are activated as a result of immunological synapse (IS) formation. To form IS productively, DCs must direct peptide–MHC complex delivery to the site of T cell contact via tu-

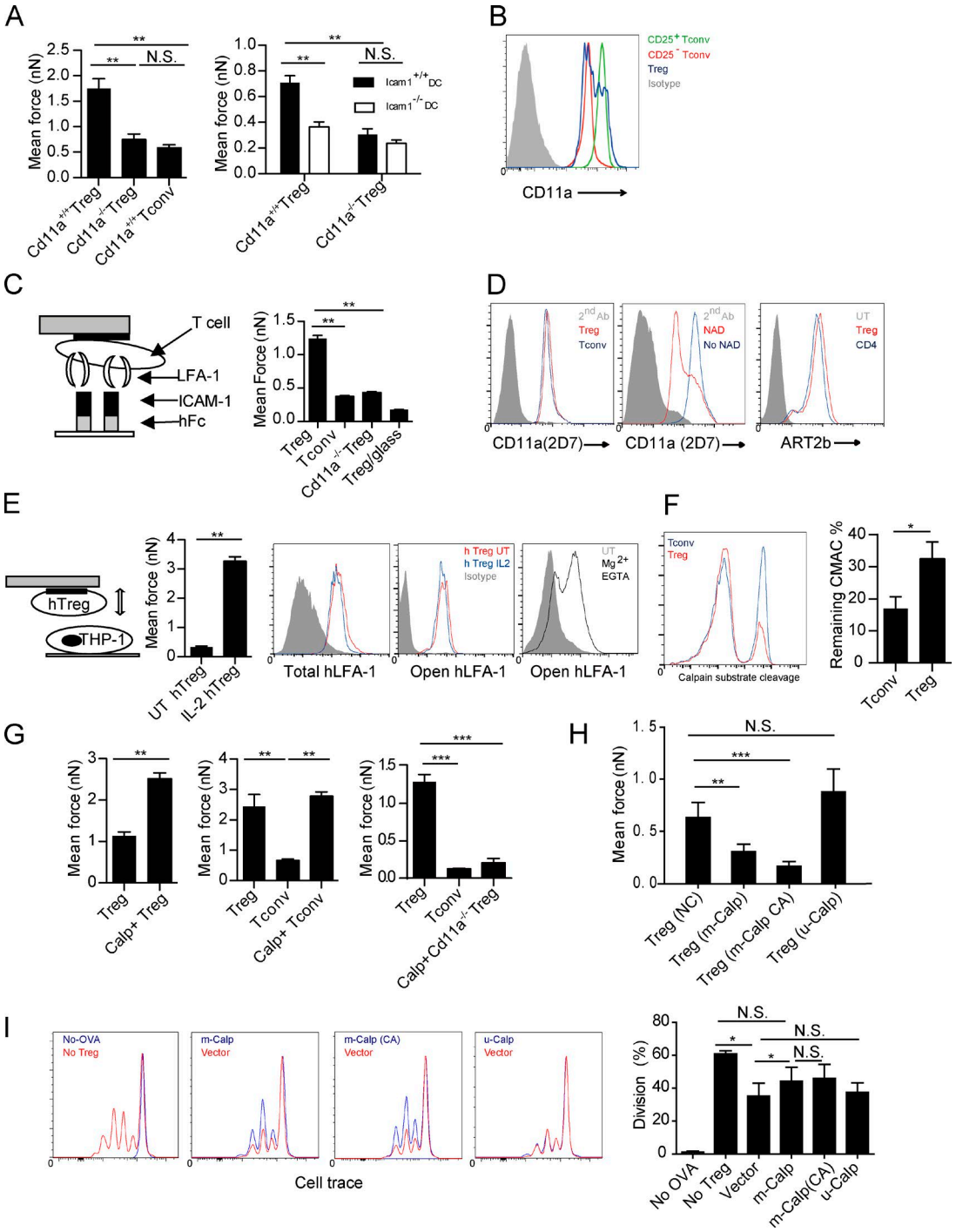

Figure 2. **An intrinsic low level of calpain is associated with the high strength binding by LFA-1 on T reg cells.** (A, left) Mean forces of wild-type or LFA-1 T-DC–deficient T reg, or T conv cells adhering to DC2.4 cells. (right) Mean forces of wild-type or LFA-1–deficient T reg cells adhering to wild-type or ICAM-1–deficient BMDCs. Representative of four independent experiments. (B) Levels of LFA-1 expression on T reg, resting ($CD25^-$), and activated ($CD25^+$) T conv cells. Representative of three independent experiments. (C, left) Schematic diagram. (right) Adhesion forces between wild-type or $Cd11a^{-/-}$ T conv or T reg cells and recombinant Fc-ICAM-1–coated on a glass slide. B6 T reg cell/blank glass contact was recorded as the background. Representative of three independent experiments. (D) ADP ribosylation of LFA-1, which is induced by NAD treatment, is known to reduce 2D7 staining intensities. (left) T reg and T conv cells were stained with 2D7 antibody without NAD treatment. (middle) The NAD treatment–induced down-regulation of 2D7 staining in comparison with the untreated control. The comparable 2D7 staining intensities on T reg cells indicate no difference in ADP-ribosylation (left). (right) Similar expression of ART2b (ART2.2), the enzyme responsible for surface LFA-1 ADP ribosylation, between T reg and T conv cells. Representative of three independent experiments. (E) Adhesion forces between IL-2–treated or untreated human T reg cells adhering to PMA-stimulated THP-1 cells grown on the disk. (left)

bular endocytic transport system (Boes et al., 2002) and simultaneously orchestrate membrane lipid reorganization and cytoskeleton polarization (Gordy et al., 2004). A network of F-actin, regulated by actin-bundling proteins, provides the essential support for such a platform on the DC side of the synapse (Al-Alwan et al., 2003). We therefore explored whether the aforementioned DC lethargy involves alteration of the DC cytoskeleton by structured illumination microscopy (SIM), which offers a resolution of ∼100 nm. We observed that whereas microtubules in DCs engaged by T reg cells were not significantly altered (Fig. 4 A), F-actin label was increased at the contact site, forming a cup-like structure embracing the T reg cell body (Fig. 4 A). Under conventional confocal microscopy with SiR-actin label, a tendency of F-actin to concentrate around T reg cell–binding site was also visible (Fig. 4 A). These observations imply that T reg cell adhesion may alter DC cytoskeleton essential for T conv binding. Cortical F-actin requires GTPase or non-GTPase bundling proteins for their structural arrangements. Although α-actinin was suggested to promote actin stress fiber association with ligated ICAM-1 (Carpén et al., 1992), it was not significantly altered in DCs upon T reg cell binding (unpublished data). Fascin-1, an actin-bundling protein only expressed in mature DCs and absent in other myeloid cells, is essential for the formation of IS involving DCs (Al-Alwan et al., 2001b; Yamakita et al., 2011). By a multistep fixation and staining protocol that best preserves actin cytoskeleton in lymphoid and myeloid cells, Fascin-1 was found to markedly cluster in patchy patterns in the proximity of T reg cell–DC contacts (Fig. 4 B). As steady contacts between untreated T conv cells and DCs were extremely rare after the fixation, we used OT-II cells in contact with OVA-pulsed DCs as the control. Although such a contact was known to accumulate Fascin-1, the degree of clustering was limited in comparison and the remaining pool of Fascin-1 in the cytosol was less disturbed (Fig. 4 B). Under T reg cell binding, Fascin-1 was clearly intermingled with actin filaments and patches, a feature more vividly revealed in individual optical sections (Fig. 4 C; Videos 1 and 2). This T reg cell–specific phenomenon was also seen when BMDCs were used (Fig. 4 D). Overall, much less Fascin-1 in DCs remained in areas away from the contact site when the DCs were bound by T reg cells than by T conv cells. When Fascin-1 was knocked down with siRNA in DCs, T reg cells could no longer bind them with strong forces (Fig. 4 E). To test whether the aggregation at the T reg cell–DC contact site limits Fascin-1 availability for supporting synapse formation with T conv cells, we overexpressed Fascin-1 in DCs. As shown in Fig. 4 E, Fascin-1 overexpression rendered DCs resistant to lethargy induced by T reg cell contacts, and such DCs were able to engage antigen-specific T conv cells with forces as strong as in unsuppressed T conv–DC pairs. Together, these data suggest that cellular Fascin-1 becomes limited in T reg cell–engaged DCs, leading to reversible DC impairment to support simultaneous synapse formation with antigen-specific T conv cells.

In some settings, brief and sequential contacts lasting several minutes between T cells and DCs are sufficient to drive T cell activation (Gunzer et al., 2000). Whether our T reg cell occupation can interfere with this type of productive engagement is not clear, as transient contacts may have more windows in the T reg cell–free state to permit short-term engagement by T cells. In other cases, to fully activate T cells into competent effector cells, the IS between T cells and DCs has to last for hours (Huppa and Davis, 2003). Although actin cytoskeleton in the T cells play a crucial role in orchestrating the IS formation, dynamic arrangement of cytoskeleton on the DC side of the IS is also required. This has been clearly demonstrated in a recent paper using AFM-based measurement that TCR signaling must be coupled to biophysical forces exerted by cytoskeleton for T cell activation (Hu and Butte, 2016). Indeed, deficiencies in cytoskeletal regulators such as Rac1/2 and WASP in DCs prohibit IS formation (Benvenuti et al., 2004; Bouma et al., 2007, 2011), and restriction in ICAM-1 lateral mobility is critical for optimal conjugation with cognate T cells (Carpén et al., 1992; Springer and Dustin, 2012). Interestingly, on individual cognate T cell/DC pairs, the binding intensity shows a trend similar to the degree of T cell activation measured by Ca^{2+} flux and IL-2 production (Lim et al., 2011). Bound by T reg cells, whether DCs freely rearrange their cytoskeleton to optimally engage T conv cells is an important question.

It should be noted that in some of our analyses, LFA-1 deficiency (unpublished data) or m-calpain overexpression did not fully remove T reg cell–mediated suppression in vivo,

Scheme. Bar graph (middle left) shows mean adhesion forces of IL-2–treated or untreated human T reg cells. Levels of total (middle) or open conformation (middle right) LFA-1 expression on IL-2-treated human T reg cells from the peripheral blood. Gray: isotype control. Human T reg cells treated with Mg^{2+} and EGTA showed elevated expression of open LFA-1 (right). Representative of three independent experiments. (F, left) T reg and T conv cells were incubated with calpain substrate CMAC; calpain activities as fluorescence signals from the digested substrate were determined by FACS after a 5-min incubation. (right) The remaining substrates were quantified. Representative of at least 10 independent experiments. (G) Mean forces of untreated or calpeptin-treated T reg cell (left), T reg or T conv (middle), and wild-type, LFA-1-deficient T reg cell, or T conv cells (right) adhering to DC2.4. Representative of five independent experiments. (H) Mean forces of vector control, m-calpain, constitutively active m-calpain, or μ-calpain–overexpressing T reg adhering to DC2.4. Representative of three independent experiments. (I) T reg cell–mediated suppression of OT-II T cell division, as measured by CellTrace dilution, stimulated by OVA-pulsed DC2.4 cells as described in the Materials and methods. (left to right) Division in the presence or absence of OVA without T reg cells; in the presence of vector transfection control or m-calpain–overexpressing T reg cells; vector or CA (constitutively active) m-calpain–overexpressing T reg cells; and vector or μ-calpain–overexpressing T reg cells. Statistical results (far right) are pooled from three independent experiments. *, $P < 0.05$; **, < 0.01; ***, < 0.001; NS, not significant.

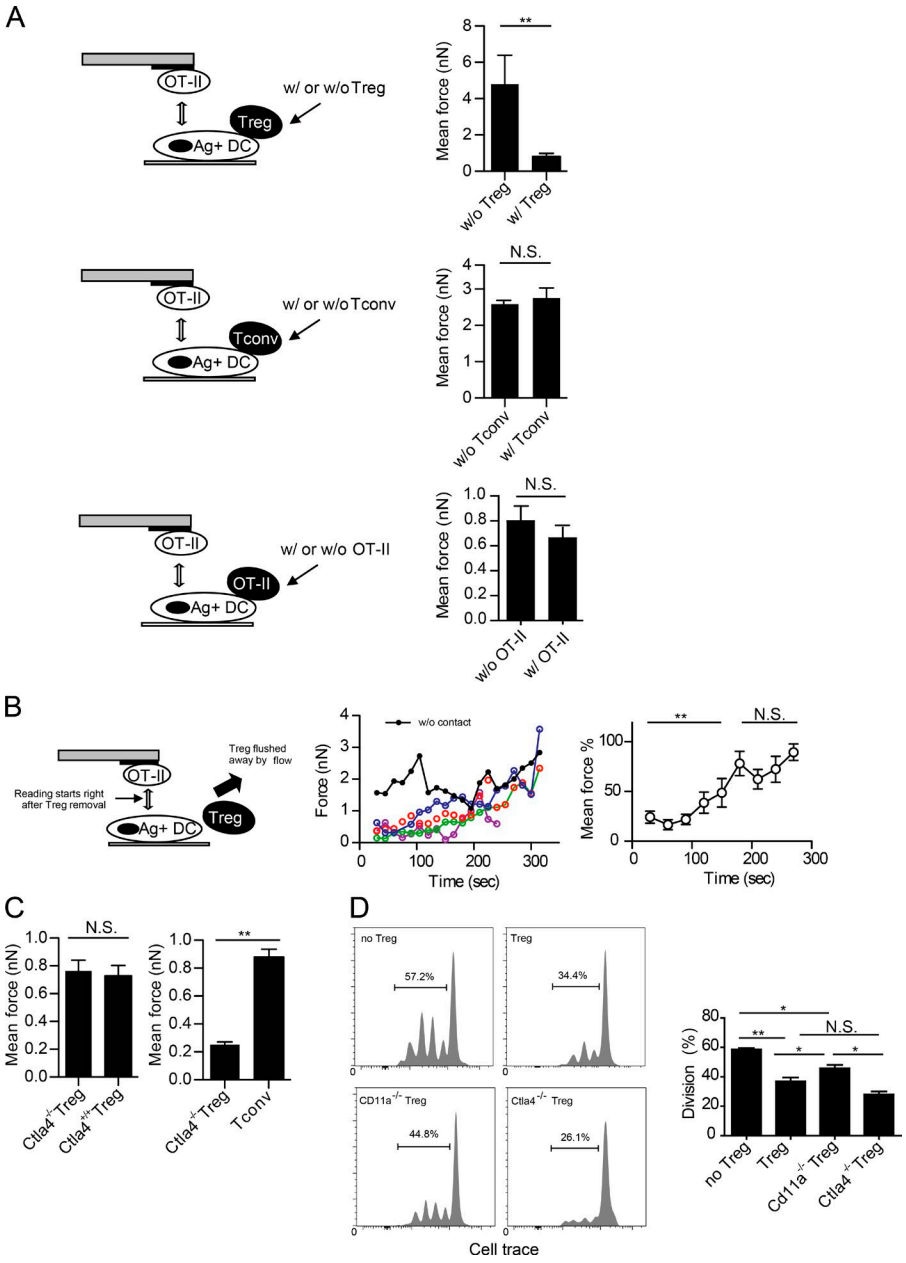

Figure 3. **T reg cell binding blocks T conv–DC interaction.** (A) Adhesion between OT-II T cells and OVA-pulsed DC2.4 cells that were free or engaged by T reg cell (top), anti-CD3/anti-CD28–activated T conv (middle), or OVA-peptide–activated OT-II T (bottom) cells on the opposite side of the DC cell bodies. Shown are the triple-cell AFM assay setup (left) and mean OT-II–DC adhesion forces (right). Each is representative of four independent experiments. (B) Adhesion between OT-II T cells and OVA-pulsed DC2.4 cells that were newly freed from engagement by T reg cells. (left) The assay setup. (middle) SCFS force readings for one control DC without prior T reg cell engagement (black) and four newly freed DCs (other colors). Time zero is the moment when the T reg cell contact was relieved by flushing. (right) The control-normalized SCFS force readings for the newly freed DCs (middle), running-averaged with a bin size of two. Representative of three independent experiments. (C, left) Mean forces of wild-type or *Ctla4*$^{-/-}$ T reg cells adhering to DC2.4 cells. (right) Mean forces of OT-II T cells adhering to OVA-pulsed DCs that were engaged on one side of the cell body by *Ctla4*$^{-/-}$ T reg cells or T conv cells. (D, left) Wild-type, *Ctla4*$^{-/-}$, and *Cd11a*$^{-/-}$ T reg cell–mediated suppression of OT-II T cell division. (right) Statistical analysis. Representative of three independent experiments. *, $P < 0.05$; **, < 0.01; NS, not significant.

suggesting that our model may be a contributing factor to the total suppressive power of T reg cells, or the tight binding is also a prerequisite for other inhibitory mechanisms. In addition, our SCFS-based techniques cannot be used to address whether T reg cells can block productive engagement between T cells and DCs in short/sequential contacts. Nevertheless, the mechanistic insight of the binding-mediated suppression in relatively long T/DC contacts is intriguing. On DCs, F-actin creates a crest like structure without constant cortical actin remodeling. This may be critical for the membrane anchoring of tubular endosomes for rapid supply of newly formed MHC/peptide complex (Boes et al., 2002) and for the inhibition of lateral diffusion of adhesion molecules. DCs are the most efficient antigen presenting cells owing not only to their prolonged endocytic digestion rate and expression of surface co-stimulatory molecules (Villadangos and Schnorrer, 2007; Mantegazza et al., 2013), but also to their unusual ability to polarize the cytoskeleton, a feature not found in macrophages and B cells (Al-Alwan et al., 2001a, 2003). This extra dimension of support may paradoxically add a layer of complexity vulnerable to regulation (Aldinucci et al., 2010). Fascin-1 is only expressed in DCs and is critically involved in the polarization (Mosialos et al., 1996; Ross et al., 2000). In the case of T reg cells, the strong polarization drains Fascin-1 to an extent whereby its availability becomes suboptimal to support other T conv activation. Overexpression of

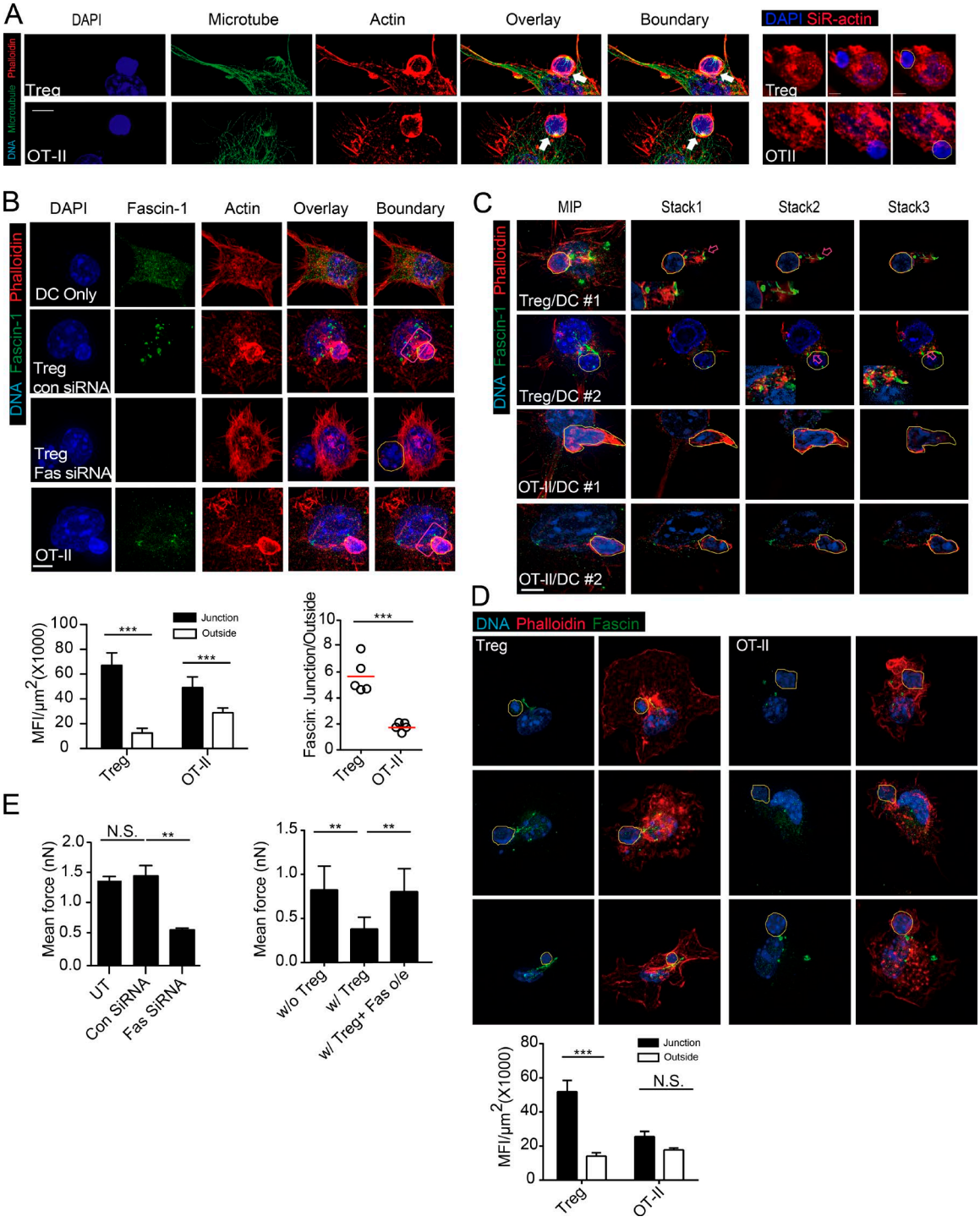

Figure 4. **Polarization of actin and DC-specific actin bundling protein.** Fascin-1 is associated with T reg cell–mediated suppression (A) Maximum-intensity projection (MIP) SIM images of a T reg cell or an OT-II T cell coupled with a DC2.4 cell pulsed with OVA, stained for DNA with DAPI, anti-α-tubulin and phalloidin. White arrows highlight the increased thickening of F-actin at the T–DC interface. Hand-traced boundaries of T cells according to DIC are shown to the right here, as well as in the subsequent images. Bars, 5 µm. Representative of at least 10 independent images from four independent stainings. (right) SiR-actin/DAPI-labeled DCs in mixture with T cells (DAPI only) under conventional microscope. (B, top) MIP SIM images of conjugates between T reg cells and DC2.4 cells transfected with control or Fascin-1 siRNA. Conjugates were stained with DAPI, phalloidin, and anti–Fascin-1 antibody. Red boxes covering the T–DC contact sites were used for statistical analyses of Facsin-1 intensity. (bottom) Fascin-1 intensities at T reg cell–DC and OT-II–DC contact sites, as indicated by red boxes in the left. (bottom right) Ratios of mean Fascin-1 intensities in and out of the junction areas. Representative of at least 10 independent images from four independent stainings. (C) MIP SIM images and representative optical sections (stack 1–3) of conjugates between T reg cell

Fascin-1 in DCs reverses this inhibition, lending credence to this scenario. It is not yet clear whether cytoskeletal changes in DCs are induced by a dedicated receptor(s) engaged by adhering T reg cells or result from the membrane biophysics of exceptionally strong adhesion. It should be noted due to the in vitro nature, this work only proposes a potential model of how T reg cells may work in vivo. The companion article by Yan et al. (2016) in this issue confirms the reduced ability of DCs to engage other cognate T cells under contact by T reg cells. That work provides the essential link to in vivo implications of our proposal. From these two angles, a scenario emerges that in addition to reported suppression mechanisms, T reg cells form a probabilistic, occupancy-based inhibitory network to reduce the spatiotemporal availability of functionally competent DCs and thereby limit the magnitude of T cell responses.

MATERIALS AND METHODS

Mice

MHC class II––deficient *H2*$^{dlAb1\text{-}Ea}$, *Cd11a*$^{-/-}$ mice, *Icam-1*$^{-/-}$ mice, and OT-II transgenic mice are maintained on the C57BL/6 background at either University of Calgary Animal Research Centre or Tsinghua University Animal Facilities. Splenocytes of *Ctla4*$^{-/-}$ mice were provided by J. Kang (University of Massachusetts Medical School, Worcester, MA). All mice were maintained under specific pathogen–free conditions, and all animal experiments were approved by the Animal Protocol Committees at University of Calgary (Alberta, Canada) and Tsinghua University (Beijing, China).

Antibodies and reagents

Anti–mouse LFA-1 antibodies clones M17 and 2D7, mouse anti–human CD11a (*Itgal*), secondary antibodies, and ELISA kits were purchased from eBioscience. PE-conjugated anti–mouse CD11a clone M17, rat anti-mouse ART2.2 clone Nika102, and mouse anti–human activated LFA-1 clone 24 were purchased from BioLegend, Novus Biologicals, Abcam, and Hycult Biotech, respectively. CD45RB antibody was obtained from BD. Lipofectamine 2000 and mouse anti–human CD4 antibodies were purchased from Invitrogen. Cell-Tak, PMA, OVA, NAD, and anti–α-tubulin antibody (DM1A) were obtained from Sigma-Aldrich. Anti–Fascin-1 antibody (55K2) was purchased from Millipore and anti–α-actinin antibody was obtained from Cell Signaling Technology. For both mouse and human T reg assays, human recombinant IL-2 (injectable clinical preparation) was used.

Cell lines and isolation of primary cells

DC2.4 and THP-1 cell lines were gifts from K. Rock (University of Massachusetts Medical School, Worcester, MA) and P. Cresswell of (Yale University, New Haven, CT), respectively. To derive DCs from the bone marrow, nonadherent marrow cells from the tibia and femur bones were cultured in the presence of 3 ng/ml GM-CSF and IL-4 for 6 d. Human peripheral blood was collected from healthy volunteers according to approved guidelines of University of Calgary, and T reg cells from these human blood samples were isolated using the human $CD4^+CD127^{low}CD49D^-CD25^+$ regulatory T cell magnetic purification kit purchased from StemCell Technologies, Inc. Murine $CD4^+CD25^+$ T reg cells and $CD4^+CD25^-$ T conv cells were isolated from spleens using magnetic purification kits from either Miltenyi Biotec or StemCell Technologies, Inc. OT-II T cells were isolated from OT-II splenocytes by Miltenyi Biotec CD4 T cell isolation kits and sometimes sorted by FACS with an anti-TCR Vα2 antibody.

siRNA transfection

Fascin-1 expression in DC2.4 cells was silenced by a pool of three siRNA (166 pmol each per T25 flask with cell densities at 70–80% confluence) delivered by Lipofectamine 2000. The siRNA oligos were synthesized by GenePharma according to our design, which was based on algorithms provided by Thermo Fisher Scientific. *Fscn1*-111, sense, 5′-CGGCAG AGGCUGUGCAGAUUU-3′, and antisense, AUCUGC ACAGCCUCUGCCGUU-3′; *Fscn1*-573, sense, 5′-CCG ACGAGAUCGCGGUAGAUU-3′, and antisense, 5′-UCU ACCGCGAUCUCGUCGGUU-3′; *Fscn1*-504, sense, 5′-CCAUGCACCCGCAGGUUAAUU-3′, and antisense, 5′-UUAACCUGCGGGUGCAUGGUU-3′. The scrambled control was also provided by Thermo Fisher Scientific.

Flow cytometry

Cells were stained with appropriate primary and secondary antibodies each for 30 min on ice with PBS washes in-between. Stained cells were analyzed directly or, occasionally, after being fixed with 1% paraformaldehyde (PFA) using FACScan, Attune, C6, or LSR II flow cytometers. Data were analyzed using FlowJo. For human LFA-1 staining, T conv and T reg cells prepared as described in Cell lines and isolation of primary cells were either untreated or treated with 100 U/ml IL-2, and then stained for human CD4 and LFA-1 in either open or closed conformation. For open conformation LFA-1^+ control, 10 mM Mg^{2+} incubation of CD4 T cells

(top two rows) or OT-II (bottom two rows) cells and DC2.4 cells. Arrows highlight areas of intermingled Fascin-1 and F-actin bundling, magnified in the inserts. Representative of at least 10 independent images from three independent stainings. (D) As in B, Fascin-1 distribution in three T reg cell–BMDC or OT-II–BMDC pairs was visualized by SIM (top) and quantitatively analyzed in the lower. Representative of three independent stainings. (E, left) Mean forces of OT-II T cells adhering to untreated, control siRNA-treated, or Fascin-1–specific siRNA-treated DC2.4 cells prepulsed with OVA. (right) Mean forces of OT-II T cells adhering to control vector-transfected or Fascin-1–overexpressing DC2.4 cells prepulsed with OVA, with or without T reg cell contact. Each is representative of at least three independent experiments. **, < 0.01; ***, < 0.001; NS, not significant.

in the presence of EGTA was performed as previously described (Dransfield and Hogg, 1989). For ADP-ribosyltransferase activity and posttranslational modification of LFA-1 epitope using M17 and 2D7 antibodies, ∼5 × 10^5 T cells were incubated with NAD at a final concentration of 30 µM for 30 min at 37°C. The cells were washed and subsequently stained for CD4 and LFA-1 with M17 and 2D7 antibodies. For measuring calpain activities, isolated T reg cells and control $CD4^+CD25^-$ cells were incubated overnight with IL-2. The cells were washed and then incubated at 100,000 cells in 200 µl media containing 0.5 µl of CMAC at 37°C and 5% CO_2 for 5 min. The cells were then immediately placed on ice and fixed with PFA to stop the reaction. The Attune was used to detect the fluorescence from converted CMAC product via the violet light channel 1.

AFM and SCFS

The experiments were performed as previously described using a JPK CellHesion unit (JPK; Flach et al., 2011). In brief, DCs were cultured on untreated glass disks. The disks were moved into an AFM-compatible chamber and mounted on to the machine stage. A clean cantilever was coated with Cell-Tak (Corning), and then used to glue individual T cells added to the disk. In each cycle, the AFM cantilever carrying a single T cell was lowered to allow T cell contact with an individual DC by 0.5–2-µm increments until the first force curve was generated. The T cell on the cantilever was then allowed to interact with the DC for 15 s before being moved upwards, until two cells were separated completely. The process was then repeated. The incubator chamber in which the machine was housed was conditioned at 37°C and at 5% CO_2. In all experiments, a minimum of 14 force curves were collected for further analysis. When raw data were analyzed, they were normalized to the background reading. To subtract the background, a blank reading (T cell contacting the glass surface) for each set of affinity measurement was collected immediately before the assay. The force curves were processed using the JPK image processing software according to the manufacturer's instructions. The line of best fit for the background data were generated first. Then all the y-values (vertical deflection) in our standard readings were corrected with the background value with the following formula: $Y = Y1 - MX + B$, where Y1 = raw data y value, M = slope obtained from background information, X = raw data × distance value, and B = the value on y-axis to move the baseline reading to 0.

To measure T–DC adhesion forces, B6, *Cd11a*$^{-/-}$, *Ctla4*$^{-/-}$ CD4 T cells, or T reg cells and human peripheral blood CD4 T/T reg cells were treated with 200 U/ml human IL-2 overnight. OT-II and T conv cells were activated by OVA 323–339 peptide, and 8 µg/ml each of anti-CD3/anti-CD28, respectively. We selected only the round and robust cells for AFM gluing, as T reg cells increase slightly in size after overnight IL-2 incubation. They also tend to have less membrane ruffling in comparison with freshly isolated T reg cells, leading to stronger gluing to silicon nitrate substrate coating on AFM tips. DC2.4 cells or BMDCs of indicated genotypes were cultured on glass disks for at least 24 h before experiments. For certain experiments, DC2.4 cells were pulsed with 100 µg/ml soluble OVA protein for 4 h. When T reg/T conv–mediated suppression of OT-II–DC adhesion was assayed, IL-2–treated T reg/T conv cells were stained with 10 µM CFSE, and DC2.4 cells were incubated with these fluorescently labeled T reg or T conv cells for ∼20 min before unlabeled OT-II T cells were added. T reg cell–DC couples identified with an UV flashlight were then approached by the cantilever tip carrying an OT-II T cell, as described in Cell lines and isolation of primary cells. For certain experiments, the T reg cell in a T reg cell–DC couple was flushed off by a micropipette tip before the freed DC was approached by the OT-II T cell for force measurement.

For each SCFS experiment, a pair of T–DC was used to generate force readings from each up and down cycle over a period of several minutes; these readings are plotted (on a fluctuating line). At least three such pairs were used for each condition. All data from these readings (at least three pairs) were used as a group for comparison among the groups, as shown in Fig. S2. This analysis is considered as one experiment. All experiments were repeated several times as indicated in the legend.

Immunostaining and SIM

DC2.4 cells were plated on sterile coverslip and treated overnight with mouse IFN-γ (50 ng/ml) and soluble OVA (100 µg/ml). When DC2.4 reached roughly 30–40% confluence, T reg cell and/or OT-II T cells were added at an approximate T/DC ratio of 2:1. After T–DC conjugate formation was ascertained with a phase-contrast microscope, media were carefully removed and cells were fixed in 2% PFA in PBS for 10 min at room temperature. For simultaneous microtubule and F-actin visualization, cells were permeabilized in acetone at −20°C before standard procedures of antibody staining. To image actin, Fascin-1 and α-actinin, the fixed cells were permeabilized with 0.5% Triton X-100-containing PBS. In contrast to the cold methanol fixation protocol recommended by the antibody manufacturer, our protocol was found to best permit simultaneous staining of both actin and microtubules, and at SIM resolution best retain the association between Fascin-1 and F-actin (Thermo Fisher Scientific).

SIM was performed with an ELYRA microscope (ZEISS), and images were processed using Zen software. To calculate the fluorescence densities, T–DC conjugates exhibiting clear contact interfaces were chosen under the confocal mode. The junctions between T reg or T conv and DCs were identified from DIC images and a box was drawn for analysis. Fascin-1 confocal images present a diffused background and are incompatible with density analysis; SIM stacks were analyzed instead, despite the reduced yields due to the complexity in data collection and analysis intrinsic to the technology. To quantitate Fascin-1 density on projection images, the pixel intensity of antibody staining was obtained with ImageJ

(National Institutes of Health). The T–DC contact junctions are approximated with boxed areas, and summed Fascin-1 intensities inside and outside of the box were normalized to their respective areas within individual DCs area. The ratio of Fascin-1 densities inside and outside of the T–DC contact junction represents the degree of polarized distribution of Fascin-1 toward the contact zone. SIM slices were taken every 0.1-µm apart, and data were presented as maximum intensity projection of all collected optical sections except that, for certain experiments as indicated, individual slices were selected to depict interactions between Fascin-1 and F-actin.

For SiR-actin labeling (a jasplakinolide-based silicon rhodamine fluorophore) for DCs, SiR-actin (Cytoskeleton, Inc.) was mixed in the media then added to DCs per the manufacturer's instructions. 1 h before the experiment, the sample was washed twice to remove free SiR-actin. T reg cell/OTII cells were then added to DCs, and the mixture was incubated for 1 h. Samples were then fixed by 2% PFA for 10 min and visualized at emission wavelength of 674 nm using confocal microscope with a 633-nm excitation laser.

Calpain and T reg cell–mediated inhibition

C57BL/6 T reg cells were stimulated on 8 µg/ml anti-CD3/anti-CD28–coated plate in the presence of 100 U/ml IL-2 2 d before infection. Wild-type mouse m- and µ-calpain cDNA were subcloned in pLVX-IRES-eGFP vector and constitutively activated calpain ST369/370/AA was generated by two-step PCR. 293FT cells in each well of 6-well plate were transfected with 2 µg pLVX plasmid, 1 µg psPAX2, and 1 µg pMD2.G with reagent (Neofect). After 48 h, the supernatant-containing lentivirus was collected, and stimulated T reg cells were infected with the lentivirus with 4 µg/ml polybrene by centrifugation at 1,500 *g* for 2 h at 32°C. 1 d after the initial infection, T reg cells were infected again with the same protocol. The resulting cells were sorted 1 d later. Purified OTII T cells were further stained by CellTrace Violet (Thermo Fisher Scientific). DC 2.4 were radiated for 70 Gy before use. 10^4 DCs, 2×10^4 OTII T cells, 1×10^4 T reg cells and 2 µM OTII peptide were mixed and cultured in each well of a 96-well U bottom plate, and were analyzed by FACS after 3 d.

Statistical analyses

Student's *t* tests were used for comparing endpoint means of different groups except that for skewed, non-Gaussian distributions of cell–cell contact duration data, the Mann-Whitney nonparametric tests were used. Data were always presented as mean ± SEM, unless indicated otherwise. Calculation and graphing were done with Prism (GraphPad). All data shown represent at least three independent experiments. *, $P < 0.05$; **, < 0.01; ***, < 0.001; NS, not significant.

Online supplemental material

Fig. S1 shows the working principles of AFM-based single force spectroscopy are described with an accompanying illustration. Fig. S2 shows how individual SCFS force measurements were collected for statistical analysis and data plot presentation. Video 1 shows heightened Fascin-1 accumulation at the site of T reg cell–BMDC contacts. Video 2 shows Fascin-1 accumulation at the site of OT-II-BMDC contacts.

ACKNOWLEDGMENTS

We thank Dr. Jim McGhee for providing SIM imaging instrument; Fei Shu and Laurie Kennedy for technical assistance; Drs. Kenneth Rock, Peter Cresswell, and Li Wu for cell lines; Dr. Joonsoo Kang for providing CTLA-4 deficient splenocytes. The Microscopy and Imaging facilities at the University of Calgary are funded by Canada Foundation for Innovation.

This work was supported by US National Institutes of Health grants (R01AI098995 and R21AI089963), Natural Sciences and Engineering Research Council of Canada grants (RGPIN-355350/396037), and a Canadian Institutes for Health Research grant (MOP-119295) to Y. Shi. P. Detampel was supported by the Swiss National Science Foundation Grant for Prospective Researchers (PBBSP3-146963).

Y. Shi and H. Qi are supported by Tsinghua-Peking Center for Life Sciences and Bayer. The authors declare no additional completing financial interest.

Submitted: 30 April 2016
Revised: 27 July 2016
Accepted: 12 December 2016

REFERENCES

Al-Alwan, M.M., G. Rowden, T.D. Lee, and K.A. West. 2001a. The dendritic cell cytoskeleton is critical for the formation of the immunological synapse. *J. Immunol.* 166:1452–1456. http://dx.doi.org/10.4049/jimmunol.166.3.1452

Al-Alwan, M.M., G. Rowden, T.D. Lee, and K.A. West. 2001b. Fascin is involved in the antigen presentation activity of mature dendritic cells. *J. Immunol.* 166:338–345. http://dx.doi.org/10.4049/jimmunol.166.1.338

Al-Alwan, M.M., R.S. Liwski, S.M. Haeryfar, W.H. Baldridge, D.W. Hoskin, G. Rowden, and K.A. West. 2003. Cutting edge: dendritic cell actin cytoskeletal polarization during immunological synapse formation is highly antigen-dependent. *J. Immunol.* 171:4479–4483. http://dx.doi.org/10.4049/jimmunol.171.9.4479

Aldinucci, A., L. Rizzetto, L. Pieri, D. Nosi, P. Romagnoli, T. Biagioli, B. Mazzanti, R. Saccardi, L. Beltrame, L. Massacesi, et al. 2010. Inhibition of immune synapse by altered dendritic cell actin distribution: a new pathway of mesenchymal stem cell immune regulation. *J. Immunol.* 185:5102–5110. http://dx.doi.org/10.4049/jimmunol.1001332

Au-Yeung, B.B., S.E. Levin, C. Zhang, L.Y. Hsu, D.A. Cheng, N. Killeen, K.M. Shokat, and A. Weiss. 2010. A genetically selective inhibitor demonstrates a function for the kinase Zap70 in regulatory T cells independent of its catalytic activity. *Nat. Immunol.* 11:1085–1092. http://dx.doi.org/10.1038/ni.1955

Benvenuti, F., S. Hugues, M. Walmsley, S. Ruf, L. Fetler, M. Popoff, V.L. Tybulewicz, and S. Amigorena. 2004. Requirement of Rac1 and Rac2 expression by mature dendritic cells for T cell priming. *Science.* 305:1150–1153. http://dx.doi.org/10.1126/science.1099159

Boes, M., J. Cerny, R. Massol, M. Op den Brouw, T. Kirchhausen, J. Chen, and H.L. Ploegh. 2002. T-cell engagement of dendritic cells rapidly rearranges MHC class II transport. *Nature.* 418:983–988. http://dx.doi.org/10.1038/nature01004

Bouma, G., S. Burns, and A.J. Thrasher. 2007. Impaired T-cell priming in vivo resulting from dysfunction of WASp-deficient dendritic cells. *Blood.* 110:4278–4284. http://dx.doi.org/10.1182/blood-2007-06-096875

Bouma, G., A. Mendoza-Naranjo, M.P. Blundell, E. de Falco, K.L. Parsley, S.O. Burns, and A.J. Thrasher. 2011. Cytoskeletal remodeling mediated by WASp in dendritic cells is necessary for normal immune synapse formation and T-cell priming. *Blood*. 118:2492–2501. http://dx.doi.org/10.1182/blood-2011-03-340265

Carpén, O., P. Pallai, D.E. Staunton, and T.A. Springer. 1992. Association of intercellular adhesion molecule-1 (ICAM-1) with actin-containing cytoskeleton and alpha-actinin. *J. Cell Biol.* 118:1223–1234. http://dx.doi.org/10.1083/jcb.118.5.1223

Cederbom, L., H. Hall, and F. Ivars. 2000. CD4+CD25+ regulatory T cells down-regulate co-stimulatory molecules on antigen-presenting cells. *Eur. J. Immunol.* 30:1538–1543. http://dx.doi.org/10.1002/1521-4141(200006)30:6<1538::AID-IMMU1538>3.0.CO;2-X

Deaglio, S., K.M. Dwyer, W. Gao, D. Friedman, A. Usheva, A. Erat, J.F. Chen, K. Enjyoji, J. Linden, M. Oukka, et al. 2007. Adenosine generation catalyzed by CD39 and CD73 expressed on regulatory T cells mediates immune suppression. *J. Exp. Med.* 204:1257–1265. http://dx.doi.org/10.1084/jem.20062512

Delgoffe, G.M., S.R. Woo, M.E. Turnis, D.M. Gravano, C. Guy, A.E. Overacre, M.L. Bettini, P. Vogel, D. Finkelstein, J. Bonnevier, et al. 2013. Stability and function of regulatory T cells is maintained by a neuropilin-1-semaphorin-4a axis. *Nature.* 501:252–256. http://dx.doi.org/10.1038/nature12428

Dransfield, I., and N. Hogg. 1989. Regulated expression of Mg2+ binding epitope on leukocyte integrin alpha subunits. *EMBO J.* 8:3759–3765.

Dustin, M.L. 2008. T-cell activation through immunological synapses and kinapses. *Immunol. Rev.* 221:77–89. http://dx.doi.org/10.1111/j.1600-065X.2008.00589.x

Flach, T.L., G. Ng, A. Hari, M.D. Desrosiers, P. Zhang, S.M. Ward, M.E. Seamone, A. Vilaysane, A.D. Mucsi, Y. Fong, et al. 2011. Alum interaction with dendritic cell membrane lipids is essential for its adjuvanticity. *Nat. Med.* 17:479–487. http://dx.doi.org/10.1038/nm.2306

Goll, D.E., V.F. Thompson, H. Li, W. Wei, and J. Cong. 2003. The calpain system. *Physiol. Rev.* 83:731–801. http://dx.doi.org/10.1152/physrev.00029.2002

Gordy, C., S. Mishra, and W. Rodgers. 2004. Visualization of antigen presentation by actin-mediated targeting of glycolipid-enriched membrane domains to the immune synapse of B cell APCs. *J. Immunol.* 172:2030–2038. http://dx.doi.org/10.4049/jimmunol.172.4.2030

Grohmann, U., C. Orabona, F. Fallarino, C. Vacca, F. Calcinaro, A. Falorni, P. Candeloro, M.L. Belladonna, R. Bianchi, M.C. Fioretti, and P. Puccetti. 2002. CTLA-4-Ig regulates tryptophan catabolism in vivo. *Nat. Immunol.* 3:1097–1101. http://dx.doi.org/10.1038/ni846

Gunzer, M., A. Schäfer, S. Borgmann, S. Grabbe, K.S. Zänker, E.B. Bröcker, E. Kämpgen, and P. Friedl. 2000. Antigen presentation in extracellular matrix: interactions of T cells with dendritic cells are dynamic, short lived, and sequential. *Immunity.* 13:323–332. http://dx.doi.org/10.1016/S1074-7613(00)00032-7

Hansen, W., M. Hutzler, S. Abel, C. Alter, C. Stockmann, S. Kliche, J. Albert, T. Sparwasser, S. Sakaguchi, A.M. Westendorf, et al. 2012. Neuropilin 1 deficiency on $CD4^{+}Foxp3^{+}$ regulatory T cells impairs mouse melanoma growth. *J. Exp. Med.* 209:2001–2016. http://dx.doi.org/10.1084/jem.20111497

Helenius, J., C.P. Heisenberg, H.E. Gaub, and D.J. Muller. 2008. Single-cell force spectroscopy. *J. Cell Sci.* 121:1785–1791. http://dx.doi.org/10.1242/jcs.030999

Herman, S., D. Krenbek, M. Klimas, M. Bonelli, C.W. Steiner, P. Pietschmann, J.S. Smolen, and C. Scheinecker. 2012. Regulatory T cells form stable and long-lasting cell cluster with myeloid dendritic cells (DC). *Int. Immunol.* 24:417–426. http://dx.doi.org/10.1093/intimm/dxs039

Hu, K.H., and M.J. Butte. 2016. T cell activation requires force generation. *J. Cell Biol.* 213:535–542. http://dx.doi.org/10.1083/jcb.201511053

Huppa, J.B., and M.M. Davis. 2003. T-cell-antigen recognition and the immunological synapse. *Nat. Rev. Immunol.* 3:973–983. http://dx.doi.org/10.1038/nri1245

Jiang, G., G. Giannone, D.R. Critchley, E. Fukumoto, and M.P. Sheetz. 2003. Two-piconewton slip bond between fibronectin and the cytoskeleton depends on talin. *Nature.* 424:334–337. http://dx.doi.org/10.1038/nature01805

Kim, C., F. Ye, and M.H. Ginsberg. 2011. Regulation of integrin activation. *Annu. Rev. Cell Dev. Biol.* 27:321–345. http://dx.doi.org/10.1146/annurev-cellbio-100109-104104

Lim, T.S., and P. Ricciardi-Castagnoli. 2012. Single-cell force spectroscopy: mechanical insights into the functional impacts of interactions between antigen-presenting cells and T cells. *Immunol. Res.* 53:108–114. http://dx.doi.org/10.1007/s12026-012-8290-x

Lim, T.S., A. Mortellaro, C.T. Lim, G.J. Hämmerling, and P. Ricciardi-Castagnoli. 2011. Mechanical interactions between dendritic cells and T cells correlate with T cell responsiveness. *J. Immunol.* 187:258–265. http://dx.doi.org/10.4049/jimmunol.1100267

Lim, T.S., J.K. Goh, A. Mortellaro, C.T. Lim, G.J. Hämmerling, and P. Ricciardi-Castagnoli. 2012. CD80 and CD86 differentially regulate mechanical interactions of T-cells with antigen-presenting dendritic cells and B-cells. *PLoS One.* 7:e45185. http://dx.doi.org/10.1371/journal.pone.0045185

Mantegazza, A.R., J.G. Magalhaes, S. Amigorena, and M.S. Marks. 2013. Presentation of phagocytosed antigens by MHC class I and II. *Traffic.* 14:135–152. http://dx.doi.org/10.1111/tra.12026

Matheu, M.P., S. Othy, M.L. Greenberg, T.X. Dong, M. Schuijs, K. Deswarte, H. Hammad, B.N. Lambrecht, I. Parker, and M.D. Cahalan. 2015. Imaging regulatory T cell dynamics and CTLA4-mediated suppression of T cell priming. *Nat. Commun.* 6:6219. http://dx.doi.org/10.1038/ncomms7219

Misra, N., J. Bayry, S. Lacroix-Desmazes, M.D. Kazatchkine, and S.V. Kaveri. 2004. Cutting edge: human CD4+CD25+ T cells restrain the maturation and antigen-presenting function of dendritic cells. *J. Immunol.* 172:4676–4680. http://dx.doi.org/10.4049/jimmunol.172.8.4676

Mosialos, G., M. Birkenbach, S. Ayehunie, F. Matsumura, G.S. Pinkus, E. Kieff, and E. Langhoff. 1996. Circulating human dendritic cells differentially express high levels of a 55-kd actin-bundling protein. *Am. J. Pathol.* 148:593–600.

Ng, G., K. Sharma, S.M. Ward, M.D. Desrosiers, L.A. Stephens, W.M. Schoel, T. Li, C.A. Lowell, C.C. Ling, M.W. Amrein, and Y. Shi. 2008. Receptor-independent, direct membrane binding leads to cell-surface lipid sorting and Syk kinase activation in dendritic cells. *Immunity.* 29:807–818. http://dx.doi.org/10.1016/j.immuni.2008.09.013

Okamoto, S., O. Azhipa, Y. Yu, E. Russo, and G. Dennert. 1998. Expression of ADP-ribosyltransferase on normal T lymphocytes and effects of nicotinamide adenine dinucleotide on their function. *J. Immunol.* 160:4190–4198.

Onishi, Y., Z. Fehervari, T. Yamaguchi, and S. Sakaguchi. 2008. $Foxp3^{+}$ natural regulatory T cells preferentially form aggregates on dendritic cells in vitro and actively inhibit their maturation. *Proc. Natl. Acad. Sci. USA.* 105:10113–10118. http://dx.doi.org/10.1073/pnas.0711106105

Paterson, A.M., S.B. Lovitch, P.T. Sage, V.R. Juneja, Y. Lee, J.D. Trombley, C.V. Arancibia-Cárcamo, R.A. Sobel, A.Y. Rudensky, V.K. Kuchroo, et al. 2015. Deletion of CTLA-4 on regulatory T cells during adulthood leads to resistance to autoimmunity. *J. Exp. Med.* 212:1603–1621. http://dx.doi.org/10.1084/jem.20141030

Qureshi, O.S., Y. Zheng, K. Nakamura, K. Attridge, C. Manzotti, E.M. Schmidt, J. Baker, L.E. Jeffery, S. Kaur, Z. Briggs, et al. 2011. Trans-endocytosis of CD80 and CD86: a molecular basis for the cell-extrinsic function of CTLA-4. *Science.* 332:600–603. http://dx.doi.org/10.1126/science.1202947

Ross, R., H. Jonuleit, M. Bros, X.L. Ross, S. Yamashiro, F. Matsumura, A.H. Enk, J. Knop, and A.B. Reske-Kunz. 2000. Expression of the actin-bundling protein fascin in cultured human dendritic cells correlates with dendritic morphology and cell differentiation. *J. Invest. Dermatol.* 115:658–663. http://dx.doi.org/10.1046/j.1523-1747.2000.00112.x

Sarris, M., K.G. Andersen, F. Randow, L. Mayr, and A.G. Betz. 2008. Neuropilin-1 expression on regulatory T cells enhances their interactions with dendritic cells during antigen recognition. *Immunity.* 28:402–413. http://dx.doi.org/10.1016/j.immuni.2008.01.012

Serra, P., A. Amrani, J. Yamanouchi, B. Han, S. Thiessen, T. Utsugi, J. Verdaguer, and P. Santamaria. 2003. CD40 ligation releases immature dendritic cells from the control of regulatory $CD4^+CD25^+$ T cells. *Immunity.* 19:877–889. http://dx.doi.org/10.1016/S1074-7613(03)00327-3

Shevach, E.M. 2009. Mechanisms of $foxp3^+$ T regulatory cell-mediated suppression. *Immunity.* 30:636–645. http://dx.doi.org/10.1016/j.immuni.2009.04.010

Springer, T.A., and M.L. Dustin. 2012. Integrin inside-out signaling and the immunological synapse. *Curr. Opin. Cell Biol.* http://dx.doi.org/10.1016/j.ceb.2011.10.004

Stewart, M.P., A. McDowall, and N. Hogg. 1998. LFA-1-mediated adhesion is regulated by cytoskeletal restraint and by a Ca2+-dependent protease, calpain. *J. Cell Biol.* 140:699–707. http://dx.doi.org/10.1083/jcb.140.3.699

Svensson, L., A. McDowall, K.M. Giles, P. Stanley, S. Feske, and N. Hogg. 2010. Calpain 2 controls turnover of LFA-1 adhesions on migrating T lymphocytes. *PLoS One.* 5:e15090. http://dx.doi.org/10.1371/journal.pone.0015090

Tadokoro, C.E., G. Shakhar, S. Shen, Y. Ding, A.C. Lino, A. Maraver, J.J. Lafaille, and M.L. Dustin. 2006. Regulatory T cells inhibit stable contacts between CD4+ T cells and dendritic cells in vivo. *J. Exp. Med.* 203:505–511. http://dx.doi.org/10.1084/jem.20050783

Tadokoro, S., S.J. Shattil, K. Eto, V. Tai, R.C. Liddington, J.M. de Pereda, M.H. Ginsberg, and D.A. Calderwood. 2003. Talin binding to integrin beta tails: a final common step in integrin activation. *Science.* 302:103–106. http://dx.doi.org/10.1126/science.1086652

Tang, Q., J.Y. Adams, A.J. Tooley, M. Bi, B.T. Fife, P. Serra, P. Santamaria, R.M. Locksley, M.F. Krummel, and J.A. Bluestone. 2006. Visualizing regulatory T cell control of autoimmune responses in nonobese diabetic mice. *Nat. Immunol.* 7:83–92. http://dx.doi.org/10.1038/ni1289

Tran, D.Q., D.D. Glass, G. Uzel, D.A. Darnell, C. Spalding, S.M. Holland, and E.M. Shevach. 2009. Analysis of adhesion molecules, target cells, and role of IL-2 in human $FOXP3^+$ regulatory T cell suppressor function. *J. Immunol.* 182:2929–2938. http://dx.doi.org/10.4049/jimmunol.0803827

Villadangos, J.A., and P. Schnorrer. 2007. Intrinsic and cooperative antigen-presenting functions of dendritic-cell subsets in vivo. *Nat. Rev. Immunol.* 7:543–555. http://dx.doi.org/10.1038/nri2103

Wing, K., Y. Onishi, P. Prieto-Martin, T. Yamaguchi, M. Miyara, Z. Fehervari, T. Nomura, and S. Sakaguchi. 2008. CTLA-4 control over Foxp3+ regulatory T cell function. *Science.* 322:271–275. http://dx.doi.org/10.1126/science.1160062

Wohler, J., D. Bullard, T. Schoeb, and S. Barnum. 2009. LFA-1 is critical for regulatory T cell homeostasis and function. *Mol. Immunol.* 46:2424–2428. http://dx.doi.org/10.1016/j.molimm.2009.04.004

Yamakita, Y., F. Matsumura, M.W. Lipscomb, P.C. Chou, G. Werlen, J.K. Burkhardt, and S. Yamashiro. 2011. Fascin1 promotes cell migration of mature dendritic cells. *J. Immunol.* 186:2850–2859. http://dx.doi.org/10.4049/jimmunol.1001667

Yan, J., B.Y. Shi, and H. Qi. 2016. Class II MHC–independent suppressive adhesion of dendritic cells by regulatory T cells in vivo. *J. Exp. Med.* 214:xxx–xxx.

Zhao, D.M., A.M. Thornton, R.J. DiPaolo, and E.M. Shevach. 2006. Activated CD4+CD25+ T cells selectively kill B lymphocytes. *Blood.* 107:3925–3932. http://dx.doi.org/10.1182/blood-2005-11-4502